



Original Paper

Exploring the synergistic effects and mechanistic insights of ionic and polyionic liquid combinations as shale inhibitors

Jia-Jun Dai^{a, b}, Kai-He Lv^{a, b, *}, Jin-Sheng Sun^{a, c}, Han Jia^{a, b}, Xian-Bin Huang^{a, b}, Jian Li^{a, b}^a Shandong Key Laboratory of Oilfield Chemistry, School of Petroleum Engineering, China University of Petroleum (East China), Qingdao, 266580, Shandong, China^b Key Laboratory of Unconventional Oil & Gas Development (China University of Petroleum (East China)), Ministry of Education, Qingdao, 266580, Shandong, China^c CNPC Engineering Technology R & D Company Limited, Beijing, 102206, China

ARTICLE INFO

Article history:

Received 24 August 2024

Received in revised form

18 February 2025

Accepted 19 February 2025

Available online 25 February 2025

Edited by Jia-Jia Fei

Keywords:

Polyionic liquids

Shale inhibitors

Clay swelling inhibition

Water-based drilling fluids

Molecular electrostatic potential

Synergistic effect

ABSTRACT

Ionic liquids (ILs), recognized for their negligible vapor pressure, thermal stability, and structural tailorability, offer targeted inhibition of clay expansion. Compared to ILs, polyionic liquids (PILs) possess stronger mechanical properties and adsorption capabilities, showing even greater potential in inhibiting clay swelling. In this work, we synthesized and characterized an imidazole-based ionic liquid (IL-NH₂), a polyionic liquid (PIL-ABHIm), and a PIL/IL combination. Their inhibitory performance was rigorously evaluated under simulated drilling conditions through immersion tests, linear swelling tests, among others. Additionally, the mechanisms underlying their interaction with clay minerals were elucidated through contact angle measurements, Fourier-transform infrared spectroscopy, X-ray diffraction (XRD), Zeta potential analysis, and molecular electrostatic potential (MEP) analysis. This work demonstrates that IL-NH₂ inhibits osmotic hydration by altering the interlayer structure of the clay, while PIL-ABHIm reduces surface hydration by forming a hydrophobic barrier on the clay surface. PIL/IL combines both mechanisms, significantly enhancing the stability of clay through the dual mechanisms of cation exchange and hydrophobic barriers. These findings reveal an innovative mechanism by which PIL/IL combination inhibits clay hydration and swelling, providing a scientific foundation for their application in drilling fluids.

© 2025 The Authors. Publishing services by Elsevier B.V. on behalf of KeAi Communications Co. Ltd. This is an open access article under the CC BY license (<http://creativecommons.org/licenses/by/4.0/>).

1. Introduction

As oil exploration and development technologies rapidly advance, the demand for drilling fluids is increasingly growing (Muhammed et al., 2021a). Water-based drilling fluids have become the most commonly used type in oil exploration and development due to their widespread applicability, environmentally friendly properties, and cost effectiveness (Gholami et al., 2018; Saleh, 2022). However, water-based drilling fluids face significant challenges in terms of wellbore stability, especially when encountering shale formations (Jiang et al., 2020, 2022; Muhammed et al., 2021b; You et al., 2014).

Shale formations are primarily composed of clay minerals, including montmorillonite, illite, and kaolinite (Wilson et al., 2016; Metwally and Chesnokov, 2012). These minerals exhibit a layered structure, with interlayer cations like sodium and calcium present

between the clay layers, capable of undergoing hydration reactions with water molecules (Swartzen-Allen and Matijevic, 1974; Anderson et al., 2010). When exposed to water-based drilling fluids, water molecules are attracted into the interlayer spaces of the clay through forces such as hydrogen bonding, leading to an increase in interlayer distance and consequently, clay volume expansion (Abbas et al., 2021). Such expansion can decrease the diameter of the drill hole, complicate drilling operations, and potentially lead to serious drilling accidents like wellbore sloughing, drill pipe sticking, or even wellbore collapse (Ahmed et al., 2020; Zamani et al., 2016; Albdiry and Almensory, 2016). Therefore, developing safe and effective shale inhibitors, especially those that mitigate the hydration and swelling of clay minerals, is crucial for enhancing wellbore stability and ensuring the safety and efficiency of drilling operations (Ma et al., 2022; Bai et al., 2023).

In recent years, ionic liquids (ILs), characterized by their unique physicochemical properties as liquid salts (Yan et al., 2019; Wang et al., 2017; Cui et al., 2016), have been recognized as ideal substitutes for traditional drilling fluid additives (Shadizadeh et al.,

* Corresponding author.

E-mail address: lkh54321@126.com (K.-H. Lv).

2015). This is attributed to their negligible vapor pressure, excellent thermal stability, customizability, and environmentally friendly attributes (Li et al., 2023). The structural tailorability of ILs, especially through the modification of cation and anion compositions as well as functional groups, allows for targeted solutions to shale stability issues, presenting broad application prospects (Rahman et al., 2020; Ahmed et al., 2019). Yang et al. have revealed that ILs with shorter alkyl chains in their ethyl imidazolium-based cations exhibit the strongest capability to inhibit clay mineral expansion (Yang et al., 2019). Additionally, Jia et al. indicated that the introduction of benzene ring structures enhances the ability of IL to cover clay mineral surfaces, thereby effectively suppressing hydration swelling (Jia et al., 2023a). These studies confirm the potential of ILs in improving shale stability and offer guidance for designing more effective ionic liquid structures. However, ILs alone face stability challenges under extreme downhole conditions, particularly at high temperatures and pressures, limiting their long-term effectiveness.

Recent studies indicate that polyionic liquids (PILs), formed through the polymerization of monomers with ionic functional groups, not only retain the low volatility, high thermal stability, and customizability of traditional ILs but also possess enhanced film-forming capabilities due to their unique polymer structure (Zhu and Yang, 2024). Tang et al. successfully prepared positively charged PIL-functionalized membranes with outstanding selective performance via simple ion exchange reactions in aqueous solutions (Tang et al., 2015). Moreover, Cowan et al. utilized PIL-IL ionogels to fabricate high-efficiency, ultrathin composite membranes for CO₂ and N₂ separation (Cowan et al., 2016). Notably, the introduction of specific functional groups into the PIL structure through molecular design significantly strengthens its interaction with clay minerals. Yang et al. found that PIL could closely envelop clay particles through multiple adsorption sites provided by imidazole groups, effectively mitigating hydration swelling (Yang et al., 2017). Dai et al. synthesized a novel PIL shale inhibitor with imidazole and trimethylamine cationic groups modified on its side chain, allowing the PIL to adhere tightly to the clay surface (Dai et al., 2024). Despite their advantages, PILs face challenges in penetrating clay layers due to their larger molecular size, which limits their effectiveness in mitigating osmotic hydration.

To address these limitations, our study explores the combination of ILs and PILs to develop a novel “dual inhibition mechanism”. This approach integrates IL’s interlayer stabilization via cation exchange with PIL’s surface hydrophobic protection through multi-point adsorption. The synergistic effect of this combination leverages the strengths of both components, aiming to provide more comprehensive shale inhibition under complex drilling conditions.

This study synthesizes a small molecule ionic liquid (IL-NH₂), a macromolecular polyionic liquid (PIL-ABHIm), and a PIL/IL combination to systematically evaluate their inhibition performance and mechanisms on shale hydration swelling. By addressing the limitations of existing shale inhibitors, we aim to enhance wellbore stability, contributing to safer and more efficient drilling operations. The effectiveness of these inhibitors was verified through experiments, and the underlying mechanisms were revealed, providing new perspectives and potential applications for the development of shale inhibitors.

2. Experimental section

2.1. Materials

2-chloroethylamine hydrochloride, 1-vinylimidazole, N,N-dimethylformamide, 2,2'-azobis(2-methylpropionitrile) and 2,2'-diallylbisphenol A were procured from Aladdin Chemistry Co., Ltd., China.

Sodium montmorillonite (Na-MMT) was used in the immersion test and the linear swelling test was obtained from Weifang Huawei Bentonite Group Co., Ltd., China. The shale used in the hot-rolling recovery test was provided by Bohai Oilfield, China. The clay mineralogical compositions of Na-MMT and the shale are detailed in Table 1.

2.2. Syntheses of IL-NH₂ and PIL-ABHIm

The synthesis processes of IL-NH₂ and PIL-ABHIm are shown in Fig. 1, specifically divided into the following two steps:

Step I: Equimolar amounts of 2-chloroethylamine hydrochloride and 1-vinylimidazole were added to a round-bottom flask containing acetonitrile. The mixture was subjected to nitrogen gas flow and heated to 80 °C, followed by reflux stirring for 24 h. After the reaction concluded, the mixture was cooled and left to settle for phase separation, yielding a deep orange liquid. This liquid was then treated with methanol and concentrated using a rotary evaporator to remove excess solvent. The final product was dried in a vacuum oven at 60 °C for 6 h, resulting in 1-aminoethyl-3-vinylimidazolium chloride (IL-NH₂) (Ren et al., 2019).

Step II: IL-NH₂ was dissolved in N,N-dimethylformamide and mixed with an appropriate amount of 2,2'-diallylbisphenol A. Then, an appropriate amount of 2,2'-azobisisobutyronitrile was added as the initiator. The mixture was reacted under a nitrogen atmosphere at 80 °C for 24 h, producing a thick brown liquid. This liquid was washed three times with ethanol and subsequently dried under vacuum at 60 °C for 6 h. The process yielded a novel shale inhibitor, designated as PIL-ABHIm (Yang et al., 2017).

Unless otherwise specified, the concentration of the shale inhibitor used in this study was 1 wt%. The concentration of the combination of PIL-ABHIm + IL-NH₂ (PIL/IL) was 1 wt%, consisting of 0.5 wt% of each component.

2.3. Characterization of IL-NH₂ and PIL-ABHIm

2.3.1. FT-IR

Fourier Transform Infrared Spectroscopy (FT-IR) analyses were performed using the ThermoScientific Nicolet IS50 Fourier Transform Infrared Spectrometer, provided by Thermo Fisher Scientific, USA. The Attenuated Total Reflectance (ATR) method was employed for the analysis. In a dry environment, the ATR accessory was initially placed in the spectrometer’s optical path. This was followed by scanning the air background. Subsequently, the sample to be tested was applied onto the crystal surface of the ATR accessory, enabling the capture of the broad spectral range of IL-NH₂ and PIL-ABHIm between 4000 and 500 cm⁻¹ (Yang et al., 2017).

2.3.2. ¹H NMR

The ¹H NMR spectra for IL-NH₂ and PIL-ABHIm were recorded using a Bruker AV400MHz NMR spectrometer, with D₂O as the solvent (Zhou et al., 2020). The spectra reference was set to the residual proton signal of the solvent. This approach ensures accurate chemical shift measurements by aligning them with a known standard, facilitating precise identification and analysis of the molecular structures of IL-NH₂ and PIL-ABHIm.

Table 1
Clay mineral compositions in Na-MMT and shale.

Mineral	Smectite, %	Illite, %	Kaolinite, %	Chlorite, %
Na-MMT	95	1	4	—
Shale	34	54	7	5

“—” denotes the absence of this component.

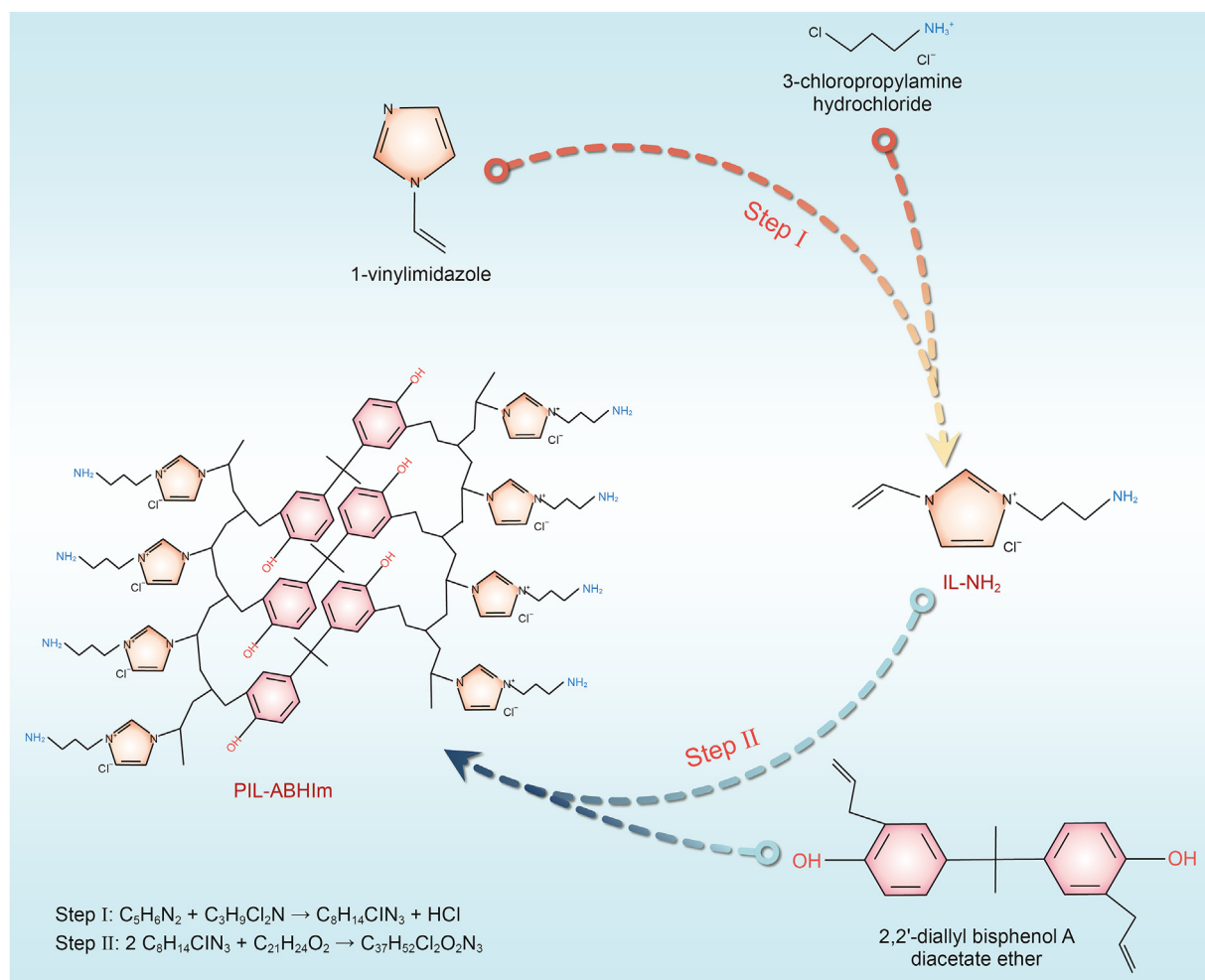


Fig. 1. The synthesis of IL-NH₂ and PIL-ABHIm.

2.3.3. Surface tension

Surface tension measurements for IL-NH₂ and PIL-ABHIm solutions at various concentrations were carried out using a BYZ-1 tensiometer. To mitigate errors associated with adsorption dynamics, samples were allowed to equilibrate for 15 min within the measurement container before the surface tension was assessed. This preparatory step ensures that the measurements accurately reflect the equilibrium surface tension values of the solutions, crucial for understanding the interfacial properties of IL-NH₂, PIL-ABHIm and PIL/IL combination in different concentrations.

2.3.4. TGA

Thermogravimetric analysis (TGA) of IL-NH₂ and PIL-ABHIm was performed with a Netzsch STA 409 PC apparatus in a nitrogen atmosphere. The temperature was ramped from 30 to 800 °C at a rate of 10 °C/min to observe the thermal decomposition characteristics of IL-NH₂, PIL-ABHIm and PIL/IL combination.

2.4. Inhibition performance

2.4.1. Immersion test

5g of Na-MMT were compressed into a pellet at 10 MPa for 5 min. The Na-MMT pellets were subsequently immersed in different inhibitor solutions and photographed at 5 min, 12 h, 24 h, and 48 h post-immersion (Jia et al., 2023b).

2.4.2. Linear swelling test

Pellets of Na-MMT were produced by compressing 10 g of Na-MMT under a pressure of 10 MPa for 8 min. The pellets were then placed in a shale expansion instrument (CPZ-II, Qingdao) containing varied inhibitor solutions. The swelling tests were conducted at room temperature (25 °C) and under standard atmospheric pressure (1 atm). For 24 h, the height of each pellet was continuously monitored (Beg et al., 2021).

2.4.3. Hot-rolling recovery test

The rock cuttings were mashed and sieved through a 6–8 mesh screen, then dried at 105 °C. 30 g of the rock-cutting samples were weighed and mixed with 350 mL of inhibitor solution and then placed into an aging jar. This sealed aging jar was subjected to a thermal rolling process for 16 h in a roller heating furnace (BRGL-7, Qingdao) at specified temperatures (90, 120, and 150 °C). After the completion of the thermal rolling, the aging jar was allowed to cool. The rock cuttings were then briefly rinsed with clean water using a 40 mesh sieve, collected on drying paper, dried again at 105 °C, and weighed. This final weight was recorded as *M*.

Eq. (1) employed to determine the hot-rolling recovery rate (*R_H*) was as follows:

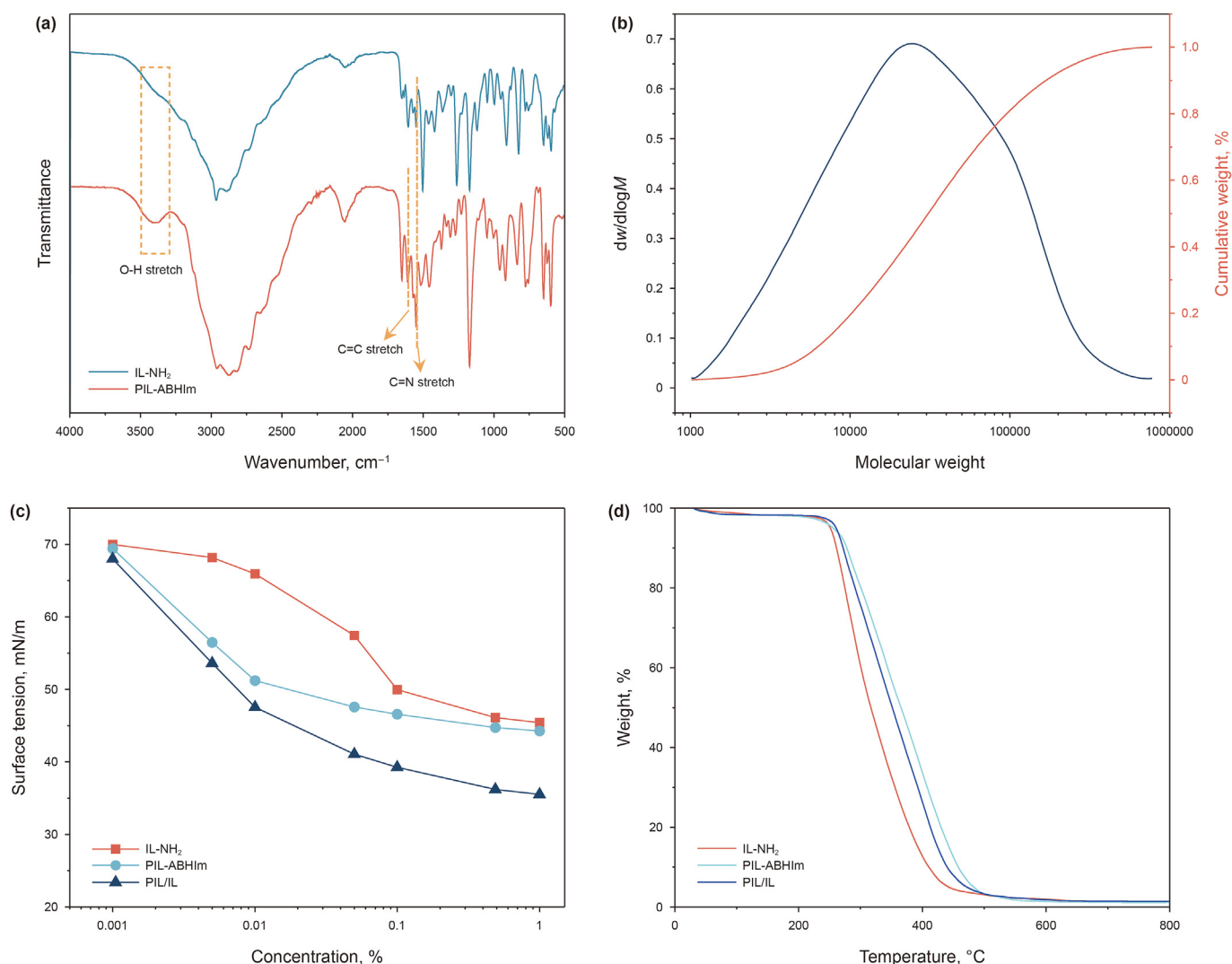


Fig. 2. Multifaceted characterization of IL-NH₂ and PIL-ABHIM via (a) FT-IR spectroscopy, (b) GPC analysis, (c) surface tension measurements, and (d) TGA analysis.

$$R_H = \frac{M}{30} \times 100\% \quad (1)$$

2.4.4. Particle size distribution measurement

Particle size distribution of Na-MMT/inhibitor mix suspensions was determined using a Malvern Mastersizer 3000 particle size analyzer. Reasonable test conditions were preset, and the sample was added to the sample pool. The SOP (standard operating procedure) test procedure was run to obtain the volume percentage of the sample across different sub-intervals within the 0.01–2000 μm range.

2.5. Inhibition mechanism analysis

Initially, a 4 wt% Na-MMT suspension was prepared with deionized water and stirred continuously for 24 h for full hydration. Various inhibitors were then added, with stirring for an additional 12 h. These treated mixtures were used to determine Zeta potential and particle size distribution. The mixture was centrifuged at 8000 rpm for 15 min, and the precipitate was washed thrice with deionized water. Finally, the precipitate, dried at 105 °C, was ground into powder for X-ray diffraction (XRD), FT-IR, and TGA.

The XRD analysis was conducted using an Empyrean X-ray generator, equipped with Cu K α radiation ($\lambda = 1.5406 \text{ \AA}$), operating at 45 kV voltage and 40 mA current. The Zeta potential of the supernatant of Na-MMT dispersion was measured using the Malvern Zetasizer Nano series. Particle size distribution was analyzed with the Malvern Mastersizer 2000. The contact angle measurements were carried out by spreading the Na-MMT suspension on a glass substrate, drying it in an oven, and then measuring the water contact angle on the glass substrate with a JC2000D5M contact angle goniometer.

Employing density functional theory as the theoretical basis, the molecular structures of IL-NH₂ and PIL-ABHIM were precisely optimized using the DMol3 module within the Materials Studio software, with the LDA and PWC functionals applied. Moreover, the electronic density and electrostatic characteristics of the molecules were calculated in detail. Ultimately, the electrostatic potentials were mapped onto the total electron density surface.

3. Results and discussion

3.1. Characterization

3.1.1. Molecular structure analysis

To characterize the chemical structures of IL-NH₂ and PIL-

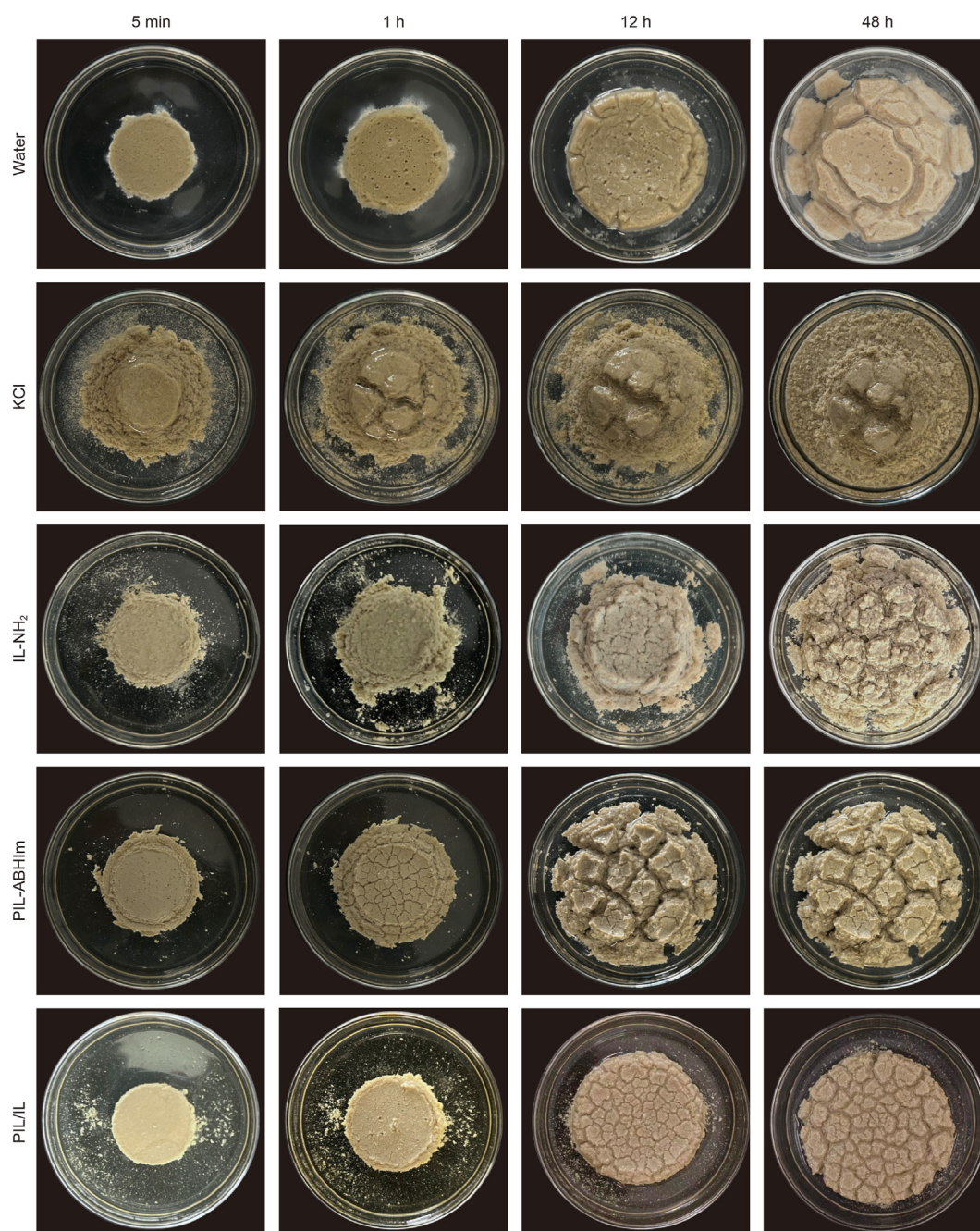


Fig. 3. Morphology of Na-MMT pellets soaked in various solutions.

ABHIm, both FTIR and ^1H NMR spectroscopy analyses are utilized. As illustrated in Fig. 2(a), the distinct absorption peaks in the range of $1500\text{--}1600\text{ cm}^{-1}$, caused by the stretching vibrations of the C=N bond, confirm the existence of the imidazole ring (Jia et al., 2023b). Additionally, the broad absorption peak between 3300 and 3500 cm^{-1} is attributed to the stretching vibrations of the O–H bond (Beg et al., 2021). The stretching vibrations of the C=C bonds in the benzene ring are typically manifested as multiple absorption peaks within $1450\text{--}1600\text{ cm}^{-1}$ range (Ren et al., 2021; Luo et al., 2017). The generation of these characteristic peaks indirectly confirms the successful synthesis of IL-NH₂ and PIL-ABHIm. The ^1H NMR spectroscopic analysis results confirm the presence of the anticipated functional groups, thereby verifying the successful synthesis of IL-NH₂ and PIL-ABHIm (Table S1).

3.1.2. Physical properties analysis

Exploring the physical properties of ionic liquids is crucial for understanding their inhibitory effects. GPC analysis determined the molecular weight and its distribution for the PIL-ABHIm, as presented in Table S2 and Fig. 2(b). The larger average molecular weight (Mn, 12574) and higher polydispersity index (PDI, 4.1125) may influence the mechanism of action of PIL-ABHIm.

Shale inhibitors with moderate surface activity can reduce the surface tension, thereby diminishing the driving force for drilling fluid penetration into shale layers (Rasool et al., 2022). The variation in surface tension of IL-NH₂, PIL-ABHIm and PIL/IL combination, shown in Fig. 2(c), demonstrates that IL-NH₂, PIL-ABHIm, and their combination all significantly reduce surface tension with increased concentrations. Notably, PIL/IL combination exhibits

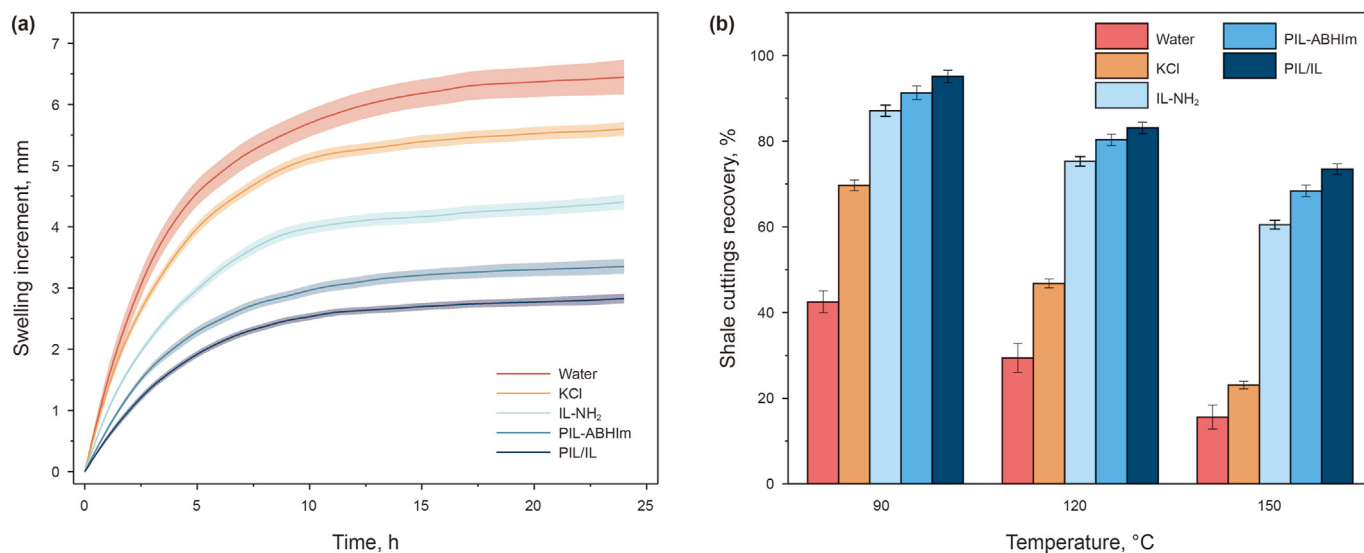


Fig. 4. (a) Swelling increments of Na-MMT pellets; (b) Recovery rates of shale cuttings after rolling at 90, 120, and 150 °C.

optimal capacity to decrease surface tension, suggesting their greatest interfacial activity.

To meet the requirements of high-temperature downhole environments, the thermal stability of IL-NH₂, PIL-ABHIm, and PIL/IL combination are investigated via the thermogravimetric analysis (Fig. 2(d)). The initial slight mass loss within the 50–100 °C range is primarily due to the evaporation of water adsorbed on the surface of the inhibitors. In the temperature range of 100–300 °C, the samples exhibit minimal weight loss, indicating their relatively stable chemical structures at these temperatures. However, as the temperature increases to 500 °C, the sample mass decreases rapidly to almost completely decompose with a residual mass less than 10%. In summary, IL-NH₂, PIL-ABHIm, and PIL/IL combination are capable of withstanding temperatures up to 300 °C.

3.2. Inhibition performance

3.2.1. Na-MMT pellets immersion test

The invasion of water-based drilling fluids into formations frequently causes the hydration and swelling of clay, thereby compromising borehole stability (Hamza et al., 2019). Immersing Na-MMT pellets in deionized water and various inhibitory solutions simulates this invasion process to evaluate the inhibitors' performance.

Fig. 3 illustrates that the surfaces of Na-MMT in deionized water initially develop fine pores and streaks as a result of water molecules diffusing inward. After prolonged immersion for 24 h, the Na-MMT pellets with edge curling and cracking undergo evident hydration and swelling to nearly four times their original volumes. Whereas the additional 5 wt% KCl results in the rapid inward collapse of Na-MMT pellets and partially inhibits their swelling, which is attributed to the ion exchange between K⁺ ions and Na⁺ ions within the montmorillonite layers. The IL-NH₂ and PIL-ABHIm exhibit greater performances than KCl in mitigating the collapse of the Na-MMT pellets. Notably, the synergistic effect of PIL/IL combination should be responsible for their superior efficacy in reducing Na-MMT swelling.

3.2.2. Linear swelling test

The linear swelling test is the most commonly used method to quantify the inhibitory performance of shale inhibitors (Saleh and

Rana, 2021; Parvizi et al., 2020). As shown in Fig. 4(a), the swelling increments of Na-MMT pellets in water, KCl (5.0 wt%), IL-NH₂ (1.0 wt%), PIL-ABHIm (1.0 wt%), and PIL/IL combination (1.0 wt %) are 6.43, 5.58, 3.10, 4.38, and 2.82 mm, respectively.

The inhibitory performances of IL-NH₂, PIL-ABHIm, and PIL/IL combination significantly surpass the efficacy of the conventional inhibitor (KCl). The lowest swelling height for the PIL/IL combination demonstrates their superior performance. The differences in inhibition effectiveness should be closely related with the molecular structures of the inhibitors and their interaction with the clay particles.

3.2.3. Hot-rolling recovery test

The shale rolling recovery experiment evaluates the impact of inhibitors on shale stability by simulating subsurface conditions (Wang, 2020; Huang et al., 2022).

As depicted in Fig. 4(b), the R_H of shale samples treated with various inhibitors significantly decrease as the temperature increases. This reduction is attributed to the accelerated penetration of water molecules into the shale structure at elevated temperatures. However, the recovery rates of IL-NH₂, PIL-ABHIm, and PIL/IL combination can achieve 60.5%, 68.4%, and 73.5% at the much high temperature (150 °C), respectively, reflecting their exceptional thermal stability. In addition, the highest recovery rate of PIL/IL combination further confirm their synergistic effect.

3.2.4. Particle size distribution measurement

The addition of shale inhibitors effectively promotes the aggregation and settling of Na-MMT suspensions, thereby enhancing shale stability and reducing the risk of wellbore collapse (Jia et al., 2023b).

Fig. 5(a) provides a direct comparison of the sedimentation of Na-MMT particles after mixing with water in the absence and presence of inhibitors for 1 and 60 min. The sample remains in suspension after treatment with water and KCl. In contrast, treatments with IL-NH₂, PIL-ABHIm, and PIL/IL combination result in clear supernatant and almost complete Na-MMT particle settling at the bottle's bottom. Particle size analysis (Fig. 5(b) and (c)) verifies the results from bottle tests, where IL-NH₂, PIL-ABHIm, and PIL/IL combination shift the peak of the particle size distribution towards larger sizes. Specifically, the D_{50} values of Na-MMT particles treated

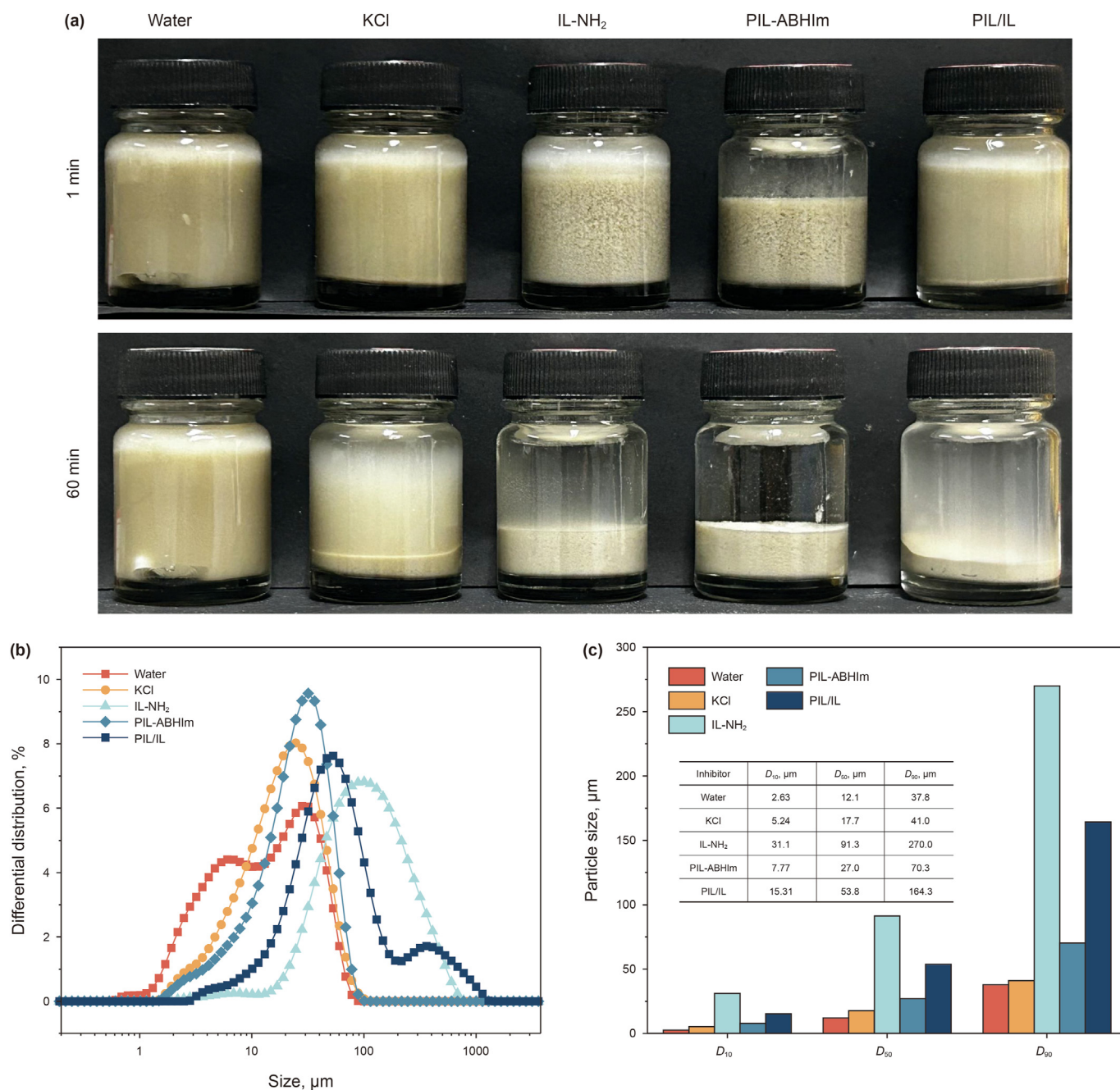


Fig. 5. Dispersion and particle size analysis of Na-MMT in various inhibitor solutions: (a) dispersion comparison at 1 and 60 min, (b) particle size distributions, (c) frequency size distribution.

with IL-NH₂ and PIL/IL combination were 270.0 and 164.3 μm , respectively, indicating their superior inhibition of clay hydration.

3.3. Inhibition mechanism analysis

3.3.1. FTIR and TGA analysis

To explore the interaction mechanisms of IL-NH₂ and PIL-ABHIm on Na-MMT, FTIR and TGA analyses are conducted on treated Na-MMT samples, as illustrated in Fig. 6(a) and (b). The Na-MMT spectrum treated with KCl is essentially identical to the original spectrum, indicating that KCl hardly interacts with Na-MMT. However, Na-MMT samples treated with IL-NH₂, PIL-

ABHIm, and PIL/IL combination exhibit characteristic C–H stretching vibration peaks at 2850 and 2919 cm^{-1} (He et al., 2020). Additionally, Na-MMT samples treated with PIL-ABHIm show slight absorption peaks between 3200 and 3000 cm^{-1} (Shadizadeh et al., 2015), attributed to the stretching vibrations of C–H bonds on benzene rings (Xu et al., 2019). The TGA results further validate that samples treated with KCl exhibit no significant difference in thermal decomposition behavior compared to the original Na-MMT, with weight loss remaining below 10%. Na-MMT samples treated with IL-NH₂, PIL-ABHIm, and the PIL/IL combination begin to decompose at temperatures above 300 °C.

The FTIR and TGA results indicate that the inhibitor effectively

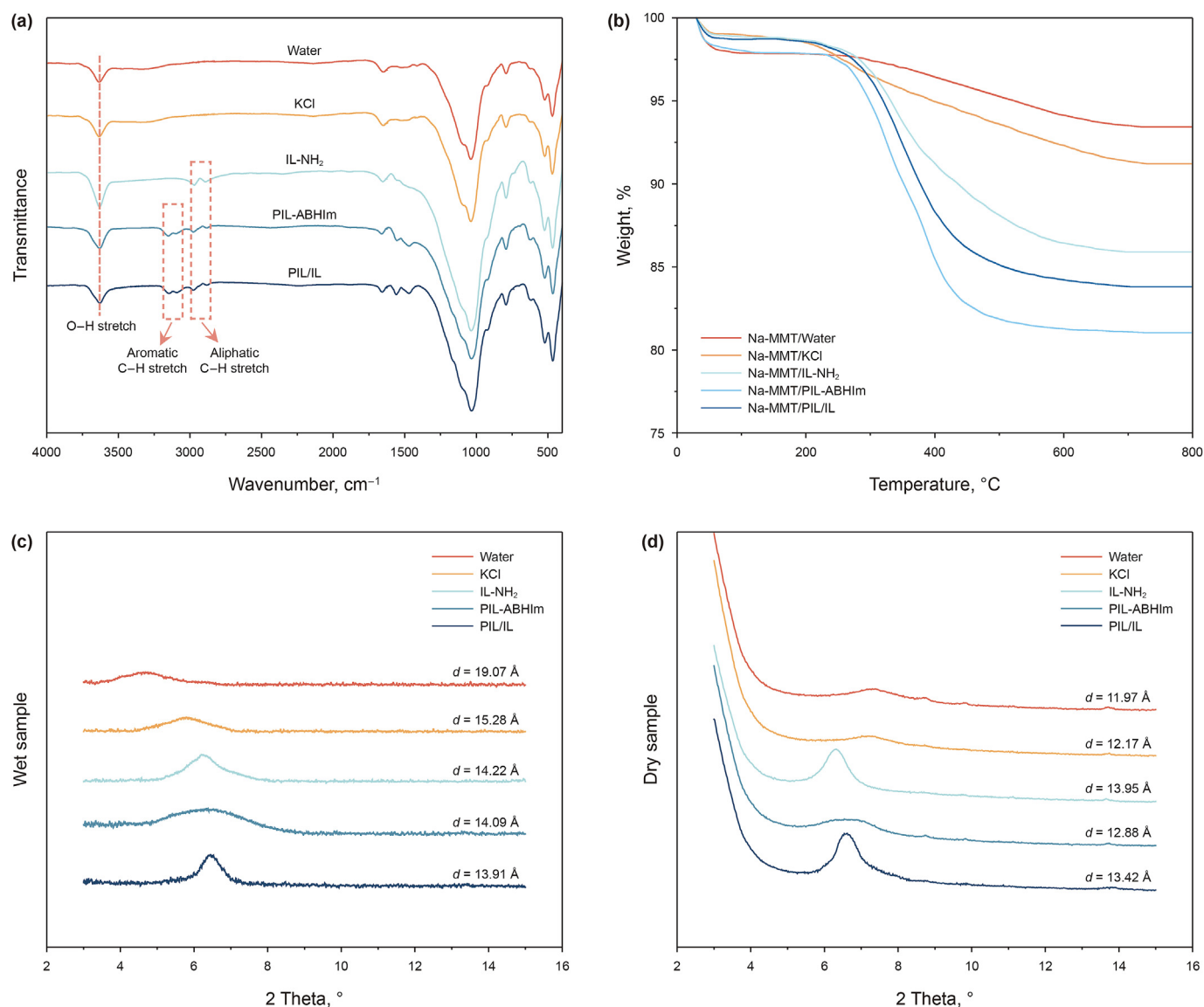


Fig. 6. Post-treatment analysis of Na-MMT: (a) FT-IR spectra, (b) thermal stability, (c) XRD spectrum of dry samples, and (d) XRD spectrum of wet samples.

interacts with Na-MMT and exhibits excellent thermal stability, making it suitable for shale inhibition in high-temperature wellbore environments.

3.3.2. XRD analysis

The changes in D-spacing (d_{001}) demonstrate the intercalation effects of inhibitors between clay layers and indirectly reveal the anti-swelling traits of the inhibitor (Rasool et al., 2022).

As illustrated in Fig. 6(c) and (d), the d_{001} values of Na-MMT samples treated with water are 11.97 Å in dry conditions and 19.07 Å in wet conditions, indicating the clay's high susceptibility to hydration-induced swelling. For the Na-MMT dry samples (Fig. 6(c)), both IL-NH₂ and PIL/IL combination expand the interlayer distance to varying extents, confirming successful cation insertion by IL-NH₂. Nevertheless, the d_{001} value of Na-MMT treated with PIL-ABHIm increases slightly, indicating that only a small portion of the oligomeric cations enters the interlayer space. For the wet samples (Fig. 6(d)), the d_{001} values for PIL-ABHIm and PIL/IL combination are all lower than those for KCl and IL-NH₂.

The above results indicated that the inhibition mechanisms of

IL-NH₂, PIL-ABHIm, and PIL/IL combination were different, which might have been due to differences in their molecular structures, surface activities, and modes of interaction with clay particles.

3.3.3. Contact angle measurement

To further investigate changes in the hydrophilicity and hydrophobicity of the clay surface, water contact angle measurements are conducted for Na-MMT samples treated with IL-NH₂, PIL-ABHIm, and PIL/IL combination (Fig. 7(a)).

The original Na-MMT surface is extremely hydrophilic, causing water droplets to spread immediately upon contact and resulting in a contact angle close to 0°. After treatment with IL-NH₂, PIL-ABHIm, and PIL/IL combination, the contact angles of the samples increased to 9.9°, 41.9°, and 28.0° respectively. This increase is primarily due to the adsorption of the inhibitor cations, which altered the hydrophobic characteristics of the Na-MMT surface. Notably, the treatment with PIL-ABHIm resulted in the highest contact angle, creating a hydrophobic layer that effectively prevents water penetration.

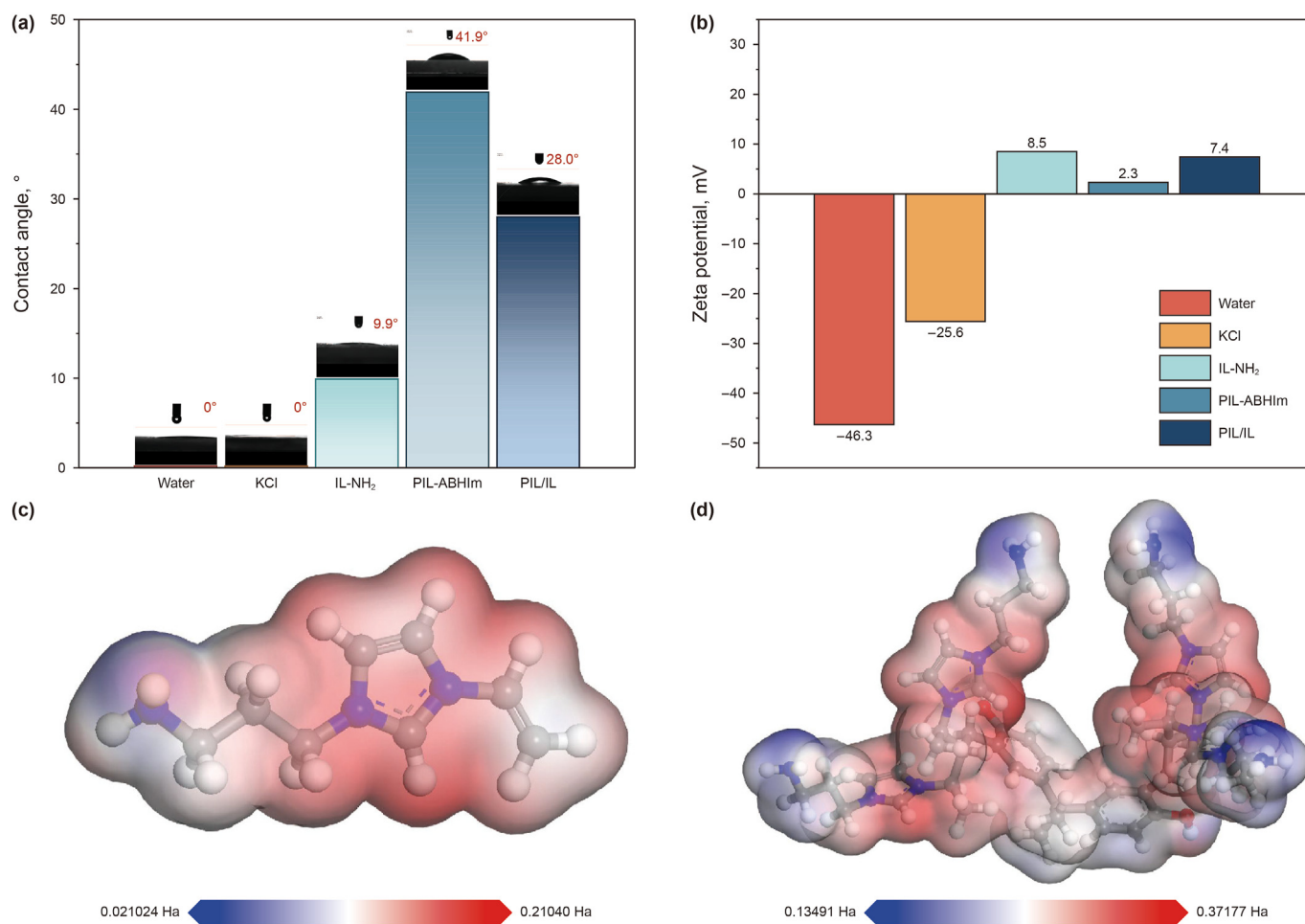


Fig. 7. Surface interactions of Na-MMT with inhibitors: (a) Contact angles, (b) Zeta potential of suspensions; (c) MEP calculation of IL-NH₂ and (d) PIL-ABHIm.

3.3.4. Zeta potential measurement

The Zeta potential is a crucial indicator of the stability of colloidal dispersions. As depicted in Fig. 7(b), Na-MMT treated with water exhibits a notably high Zeta potential of -46.3 mV, indicating the suspension's superior stability (Fig. 5(a)). The addition of KCl reduces the Zeta potential to -25.6 mV, compressing the clay's double layer and leading to particle aggregation, which helps suppress clay expansion. Furthermore, treatment with IL-NH₂, PIL-ABHIm, and PIL/IL combination shifts the Zeta potential of Na-MMT to positive values of 8.5, 2.3, and 7.4 mV, respectively. This shift is attributed to the adsorption of IL-NH₂ and PIL-ABHIm onto the clay surface via electrostatic forces and hydrogen bonding, effectively reducing the Zeta potential.

Additional Zeta potential measurements for drilling fluids (Fig. S1) show minimal changes with the addition of IL-NH₂, PIL-ABHIm, and the PIL/IL combination, maintaining values close to the base mud (-42.3 mV). This demonstrates that the inhibitors do not compromise the stability of the drilling fluid system, supporting their compatibility for field applications.

3.3.5. MEP distribution

The electrostatic potential of molecules, visualized through simulations on the surface of shale inhibitor molecules, is a crucial way to understanding their interactions with clay (Ahmed et al., 2019).

Fig. 7(c) and (d) depict the electrostatic potential distribution of IL-NH₂ and PIL-ABHIm, respectively. Red areas signify lower

electron density, increasing susceptibility to nucleophilic attacks, and blue areas indicate higher electron density, making them prone to electrophilic attacks (Weigend and Ahlrichs, 2005). Protonation of amine and imidazole groups enhances the adsorption of IL-NH₂ and PIL-ABHIm on clay. Additionally, the potential of PIL-ABHIm (0.37177 Ha) exceeds that of IL-NH₂ (0.21040 Ha), indicating that PIL-ABHIm adsorbs more effectively onto the clay surface through electrostatic interactions (Fig. 7(a)).

3.4. Inhibition mechanism

Based on the mechanistic analysis of the experimental results, we propose potential mechanistic explanations for both IL-NH₂, PIL-ABHIm and PIL/IL combination. Fig. 8(a) illustrates that upon contact between clay and water, water molecules initially adsorb on its negatively charged surfaces and around the interlayer Na⁺ ions, leading to surface hydration. Over time, an increasing number of attracted water molecules penetrate into the interlayers, known as osmotic hydration, which further enlarges the interlayer distance. Furthermore, the high cation exchange capacity of clay facilitates the influx of more water molecules into the interlayer space, leading to significant expansion of clay.

In past studies, the inhibition mechanisms of shale inhibitors primarily include cation exchange, encapsulation, and electrostatic effects (Rana et al., 2019; Wei et al., 2024). The imidazolium cation in our prepared small molecule ionic liquid IL-NH₂ can exchange with cations between clay layers, leading to an increase in the

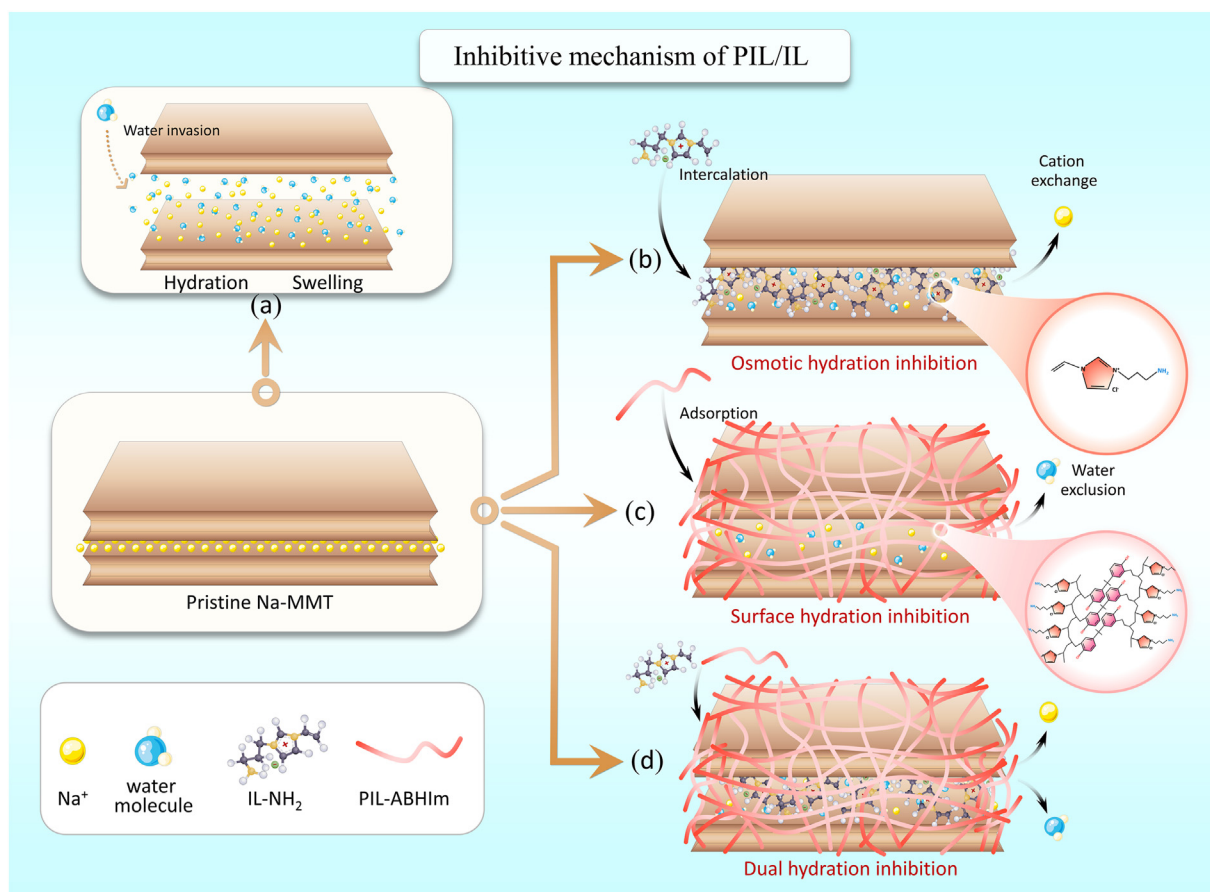


Fig. 8. Diagram of the inhibitive mechanisms on Na-MMT: (a) Swelling of Na-MMT without inhibitors, (b) Inhibition by IL-NH₂ through osmotic hydration reduction, (c) Inhibition by PIL-ABHIm through surface hydration reduction, (d) Inhibition by PIL/IL combination through dual hydration inhibition.

interlayer spacing of Na-MMT dry samples (Fig. 6(c) and 8(b)). The imidazolium cation densely fills the interlayer space, restricting the entry of water molecules and thereby reducing osmotic hydration. Additionally, the cations interact with the negative charges on the clay surface, lowering the system's Zeta potential and weakening the electrostatic repulsion between clay particles (Fig. 7(b)), making the clay particles more prone to aggregation (Fig. 5(a)), effectively reducing hydration expansion.

Due to the larger molecular structure of polyionic liquid PIL-ABHIm, it cannot enter the Na-MMT interlayer (Fig. 2(b) and 6(c)). Instead, MEP distribution reveals that polymer cations with high potentials, such as imidazolium and amine groups, form stable multi-point hydrogen bonds with hydroxyl groups on the clay surface (Fig. 7(d)). This surface adsorption mechanism was further validated through contact angle measurements, which showed significant increases in hydrophobicity, particularly in PIL-ABHIm-treated samples (Fig. 7(a)). These bonds firmly adsorb PIL-ABHIm onto the clay surface, enhancing the overall stability of the clay and simultaneously forming a hydrophobic barrier, reducing surface hydration.

Through synergistic effects and multiple complementary mechanisms, PIL/IL can not only change the interlayer structure of the clay and reduce osmotic hydration of water molecules in the clay layers, but also form a hydrophobic barrier on the clay surface, reducing surface hydration of water molecules, and exhibiting optimal inhibitory effects (Fig. 8(d)).

4. Conclusions

This study evaluated the inhibition performance and mechanisms of IL-NH₂, PIL-ABHIm, and PIL/IL combination on shale hydration swelling. The experimental results showed that PIL/IL combination significantly reduced the linear expansion height to 2.82 mm and achieved a hot-rolling recovery rate of up to 73.5% at 150 °C, demonstrating superior inhibition capability compared to any single inhibitor. Mechanism experiments revealed that IL-NH₂ inhibits penetrative hydration by altering the clay interlayer structure through cation exchange, while PIL-ABHIm forms a hydrophobic barrier with multiple adsorption sites, enhancing the hydrophobicity of the clay surface and reducing surface hydration. The PIL/IL combination integrates these two mechanisms, significantly enhancing clay stability through both cation exchange and hydrophobic barrier formation. This study is the first to combine small molecule ionic liquids (IL-NH₂) and macromolecular polyionic liquids (PIL-ABHIm) for shale inhibition, proposing a novel dual inhibition mechanism. The results highlight the significant application potential of the PIL/IL system, offering an innovative approach to address the challenges of shale hydration and swelling. Compared to conventional inhibitors, this system achieves better performance with a lower dosage (1 wt%), making it more efficient and potentially more cost-effective in practical applications.

Additionally, this study provides valuable insights into the molecular-level interactions between inhibitors and clay, which

could guide the design of more advanced shale inhibitors. While this study focuses on controlled laboratory conditions, the findings offer a strong basis for further exploration. Future studies can focus on optimizing the formulation and validating the performance under diverse field conditions to facilitate its industrial application.

In summary, this study provides insights into the dual inhibition mechanism of PIL/IL and a framework for next-generation shale inhibitors, advancing efficient and sustainable drilling technologies.

CRediT authorship contribution statement

Jia-Jun Dai: Writing – review & editing, Writing – original draft, Validation, Data curation. **Kai-He Lv:** Writing – original draft, Resources, Funding acquisition. **Jin-Sheng Sun:** Resources, Funding acquisition. **Han Jia:** Writing – review & editing, Investigation. **Xian-Bin Huang:** Supervision, Methodology. **Jian Li:** Validation, Investigation.

Declaration of interest statement

The authors declare that they have no known competing financial interests or personal relationships that could have appeared to influence the work reported in this paper.

Acknowledgements

The authors are grateful for funding from the National Natural Science Foundation of China (Nos. 51991361 and 52288101) and the Young Scientists Fund of the National Natural Science Foundation (No. 52204023).

Appendix A. Supplementary data

Supplementary data to this article can be found online at <https://doi.org/10.1016/j.petsci.2025.02.012>.

References

- Abbas, M.A., Zamir, A., Elraies, K.A., et al., 2021. A critical parametric review of polymers as shale inhibitors in water-based drilling fluids. *J. Pet. Sci. Eng.* 204, 108745. <https://doi.org/10.1016/j.petrol.2021.108745>.
- Ahmed, H.M., Kamal, M.S., Al-Harhi, M., 2019. Polymeric and low molecular weight shale inhibitors: a review. *Fuel* 251, 187–217. <https://doi.org/10.1016/j.fuel.2019.04.038>.
- Ahmed, K.R., Murtaza, M., Abdurraheem, A., et al., 2020. Imidazolium-based ionic liquids as clay swelling inhibitors: mechanism, performance evaluation, and effect of different anions. *ACS Omega* 5 (41), 26682–26696. <https://doi.org/10.1021/acsomega.0c03560>.
- Albdiry, M.T., Almensory, M.F., 2016. Failure analysis of drillstring in petroleum industry: a review. *Eng. Fail. Anal.* 65, 74–85. <https://doi.org/10.1016/j.engfailanal.2016.03.014>.
- Anderson, R.L., Ratcliffe, I., Greenwell, H.C., et al., 2010. Clay swelling—a challenge in the oilfield. *Earth Sci. Rev.* 98 (3–4), 201–216. <https://doi.org/10.1016/j.earscirev.2009.11.003>.
- Bai, J., Feng, X., Chen, Z.W., et al., 2023. Investigation of the mechanism and effect of citric acid-based deep eutectic solvents inhibiting hydration and expansion of gas shale clay minerals. *Energy Fuels* 37 (4), 2750–2758. <https://doi.org/10.1021/acs.energyfuels.2c03819>.
- Beg, M., Haider, M.B., Thakur, N.K., et al., 2021. Clay-water interaction inhibition using amine and glycol-based deep eutectic solvents for efficient drilling of shale formations. *J. Mol. Liq.* 340, 117134. <https://doi.org/10.1016/j.molliq.2021.117134>.
- Cowan, M.G., Gin, D.L., Noble, R.D., 2016. Poly (ionic liquid)/ionic liquid ion-gels with high “free” ionic liquid content: platform membrane materials for CO₂/light gas separations. *Acc. Chem. Res.* 49 (4), 724–732. <https://doi.org/10.1021/acs.accounts.5b00547>.
- Cui, G.K., Wang, J.J., Zhang, S.J., 2016. Active chemisorption sites in functionalized ionic liquids for carbon capture. *Chem. Soc. Rev.* 45 (15), 4307–4339. <https://doi.org/10.1039/C5CS00462D>.
- Dai, Z.W., Sun, J.S., Xiu, Z.Y., et al., 2024. Preparation and performance evaluation of ionic liquid copolymer shale inhibitor for drilling fluid gel system. *Gels* 10 (2), 96. <https://doi.org/10.3390/gels10020096>.

- Gholami, R., Elochukwu, H., Fakhari, N., et al., 2018. A review on borehole instability in active shale formations: interactions, mechanisms and inhibitors. *Earth Sci. Rev.* 177, 2–13. <https://doi.org/10.1016/j.earscirev.2017.11.002>.
- Hamza, A., Shamlooh, M., Hussein, I.A., et al., 2019. Polymeric formulations used for loss circulation materials and wellbore strengthening applications in oil and gas wells: a review. *J. Pet. Sci. Eng.* 180, 197–214. <https://doi.org/10.1016/j.petrol.2019.05.022>.
- He, Y., Zhou, L.H., Gou, S.H., et al., 2020. Synergy of imidazolium ionic liquids and flexible anionic polymer for controlling facilely montmorillonite swelling in water. *J. Mol. Liq.* 317, 114261. <https://doi.org/10.1016/j.molliq.2020.114261>.
- Huang, X.B., Sun, J.S., Li, H., et al., 2022. Fabrication of a hydrophobic hierarchical surface on shale using modified nano-SiO₂ for strengthening the wellbore wall in drilling engineering. *Engineering* 11, 101–110. <https://doi.org/10.1016/j.eng.2021.05.021>.
- Jia, H., Jia, H.D., Wang, Q.X., et al., 2023a. Investigation of dihydroxyl ionic liquids as high-performance shale inhibitors and their inhibition mechanism. *Colloids Surf., A* 662, 130999. <https://doi.org/10.1016/j.colsurfa.2023.130999>.
- Jia, H., Wei, X., Wang, Q.X., et al., 2023b. Investigation of the effects of functional groups on the inhibition performances of imidazolium-based bola-form ionic liquids as novel high-performance shale inhibitors. *Energy Fuels* 37 (14), 10585–10593. <https://doi.org/10.1021/acs.energyfuels.3c01769>.
- Jiang, G.C., Ni, X.X., Yang, L.L., et al., 2020. Synthesis of superamphiphobic nanofluid as a multi-functional additive in oil-based drilling fluid, especially the stabilization performance on the water/oil interface. *Colloids Surf., A* 588, 124385. <https://doi.org/10.1016/j.colsurfa.2019.124385>.
- Jiang, G.C., Sun, J.S., He, Y.B., et al., 2022. Novel water-based drilling and completion fluid technology to improve wellbore quality during drilling and protect unconventional reservoirs. *Engineering* 18, 129–142. <https://doi.org/10.1016/j.eng.2021.11.014>.
- Li, X.Q., Chen, K., Guo, R.L., et al., 2023. Ionic liquids functionalized MOFs for adsorption. *Chem. Rev.* 123 (16), 10432–10467. <https://doi.org/10.1021/acs.chemrev.3c00248>.
- Luo, Z.H., Wang, L.X., Yu, P.Z., et al., 2017. Experimental study on the application of an ionic liquid as a shale inhibitor and inhibitive mechanism. *Appl. Clay Sci.* 150, 267–274. <https://doi.org/10.1016/j.clay.2017.09.038>.
- Ma, J.Y., Xie, B., An, Y.X., 2022. Advanced developments in low-toxic and environmentally friendly shale inhibitor: a review. *J. Pet. Sci. Eng.* 208, 109578. <https://doi.org/10.1016/j.petrol.2021.109578>.
- Metwally, Y.M., Chesnokov, E.M., 2012. Clay mineral transformation as a major source for authigenic quartz in thermo-mature gas shale. *Appl. Clay Sci.* 55, 138–150. <https://doi.org/10.1016/j.clay.2011.11.007>.
- Muhammed, N.S., Olayiwola, T., Elkatatny, S., et al., 2021a. A review on clay chemistry, characterization and shale inhibitors for water-based drilling fluids. *J. Pet. Sci. Eng.* 206, 109043. <https://doi.org/10.1016/j.petrol.2021.109043>.
- Muhammed, N.S., Olayiwola, T., Elkatatny, S., et al., 2021b. Insights into the application of surfactants and nanomaterials as shale inhibitors for water-based drilling fluid: a review. *J. Nat. Gas Sci. Eng.* 92, 103987. <https://doi.org/10.1016/j.jngse.2021.103987>.
- Parvizi, G.S., Khodapanah, E., Tabatabaei-Nezhad, S.A., 2020. Experimental evaluation of thiamine as a new clay swelling inhibitor. *Pet. Sci.* 17 (6), 1616–1633. <https://doi.org/10.1007/s12182-020-00466-6>.
- Rahman, M.T., Negash, B.M., Moniruzzaman, M., et al., 2020. An overview on the potential application of ionic liquids in shale stabilization processes. *J. Nat. Gas Sci. Eng.* 81, 103480. <https://doi.org/10.1016/j.jngse.2020.103480>.
- Rana, A., Arfaj, M.K., Saleh, T.A., 2019. Advanced developments in shale inhibitors for oil production with low environmental footprints—a review. *Fuel* 247, 237–249. <https://doi.org/10.1016/j.fuel.2019.03.006>.
- Rasool, M.H., Ahmad, M., Ayoub, M., et al., 2022. A review of the usage of deep eutectic solvents as shale inhibitors in drilling mud. *J. Mol. Liq.* 361, 119673. <https://doi.org/10.1016/j.molliq.2022.119673>.
- Ren, Y.J., Wang, H.N., Ren, Z.C., et al., 2019. Adsorption of imidazolium-based ionic liquid on sodium bentonite and its effects on rheological and swelling behaviors. *Appl. Clay Sci.* 182, 105248. <https://doi.org/10.1016/j.clay.2019.105248>.
- Ren, Y.J., Zhai, Y.F., Wu, L.S., et al., 2021. Amine- and alcohol-functionalized ionic liquids: inhibition difference and application in water-based drilling fluids for wellbore stability. *Colloids Surf., A* 609, 125678. <https://doi.org/10.1016/j.colsurfa.2020.125678>.
- Saleh, T.A., 2022. Experimental and analytical methods for testing inhibitors and fluids in water-based drilling environments. *TrAC-Trends Anal. Chem.* 149, 116543. <https://doi.org/10.1016/j.trac.2022.116543>.
- Saleh, T.A., Rana, A., 2021. Surface-modified biopolymer as an environment-friendly shale inhibitor and swelling control agent. *J. Mol. Liq.* 342, 117275. <https://doi.org/10.1016/j.molliq.2021.117275>.
- Shadizadeh, S.R., Moslemizadeh, A., Dezaki, A.S., 2015. A novel nonionic surfactant for inhibiting shale hydration. *Appl. Clay Sci.* 118, 74–86. <https://doi.org/10.1016/j.clay.2015.09.006>.
- Swartzten-Allen, S.L., Matijevic, E., 1974. Surface and colloid chemistry of clays. *Chem. Rev.* 74 (3), 385–400. <https://doi.org/10.1021/cr60289a004>.
- Tang, Y., Tang, B.B., Wu, P.Y., 2015. Preparation of a positively charged nanofiltration membrane based on hydrophilic–hydrophobic transformation of a poly (ionic liquid). *J. Mater. Chem. A* 3 (23), 12367–12376. <https://doi.org/10.1039/C5TA01823D>.
- Wang, B.S., Qin, L., Mu, T.C., et al., 2017. Are ionic liquids chemically stable? *Chem. Rev.* 117 (10), 7113–7131. <https://doi.org/10.1021/acs.chemrev.6b00594>.
- Wang, L., 2020. Clay stabilization in sandstone reservoirs and the perspectives for

- shale reservoirs. *Adv. Colloid Interface Sci.* 276, 102087. <https://doi.org/10.1016/j.cis.2019.102087>.
- Weigend, F., Ahlrichs, R., 2005. Balanced basis sets of split valence, triple zeta valence and quadruple zeta valence quality for H to Rn: design and assessment of accuracy. *Phys. Chem. Chem. Phys.* 7 (18), 3297–3305. <https://doi.org/10.1039/B508541A>.
- Wei, Z.J., Wang, M.S., Shan, W.J., et al., 2024. Synergistic effects of potassium alginate and silicates co-inhibition performance in shale hydration. *J. Mol. Liq.* 393, 123538. <https://doi.org/10.1016/j.molliq.2023.123538>.
- Wilson, M.J., Shaldybin, M.V., Wilson, L., 2016. Clay mineralogy and unconventional hydrocarbon shale reservoirs in the USA. I. Occurrence and interpretation of mixed layer R3 ordered illite/smectite. *Earth Sci. Rev.* 158, 31–50. <https://doi.org/10.1016/j.earscirev.2016.04.004>.
- Xu, J.G., Qiu, Z.S., Zhao, X., et al., 2019. Study of 1-Octyl-3-methylimidazolium bromide for inhibiting shale hydration and dispersion. *J. Pet. Sci. Eng.* 177, 208–214. <https://doi.org/10.1016/j.petrol.2019.02.064>.
- Yan, X.R., Anguille, S., Bendahan, M., et al., 2019. Ionic liquids combined with membrane separation processes: a review. *Sep. Purif. Technol.* 222, 230–253. <https://doi.org/10.1016/j.seppur.2019.03.103>.
- Yang, L.L., Jiang, G.C., Shi, Y.W., et al., 2017. Application of ionic liquid and polymeric ionic liquid as shale hydration inhibitors. *Energy Fuels* 31 (4), 4308–4317. <https://doi.org/10.1021/acs.energyfuels.7b00272>.
- Yang, L.L., Yang, X., Wang, T.D., et al., 2019. Effect of alkyl chain length on shale hydration inhibitive performance of vinylimidazolium-based ionic liquids. *Ind. Eng. Chem. Res.* 58 (20), 8565–8577. <https://doi.org/10.1021/acs.iecr.9b01016>.
- You, L.J., Kang, Y.L., Chen, Z.X., et al., 2014. Wellbore instability in shale gas wells drilled by oil-based fluids. *Int. J. Rock Mech. Min. Sci.* 72, 294–299. <https://doi.org/10.1016/j.ijrmms.2014.08.017>.
- Zamani, S.M., Hassanzadeh-Tabrizi, S.A., Sharifi, H., 2016. Failure analysis of drill pipe: a review. *Eng. Fail. Anal.* 59, 605–623. <https://doi.org/10.1016/j.engfailanal.2015.10.012>.
- Zhou, L.H., He, Y., Gou, S.H., et al., 2020. Efficient inhibition of montmorillonite swelling through controlling flexibly structure of piperazine-based polyether Gemini quaternary ammonium salts. *Chem. Eng. J.* 383, 123190. <https://doi.org/10.1016/j.cej.2019.123190>.
- Zhu, M.Y., Yang, Y., 2024. Poly (ionic liquid): an emerging platform for green chemistry. *Green Chem.* 26, 5022–5102. <https://doi.org/10.1039/D4GC00202D>.